Electronic Supplementary Material (ESI) for RSC Advances.

Supporting Information

Active control of salinity-based power generation in nanopore using thermal and pH effects

Van-Phung Mai, Ruey-Jen Yang*

Department of Engineering Science, National Cheng Kung University, Tainan, Taiwan

Corresponding author: Prof. Ruey-Jen Yang. Email: rjyang@mail.ncku.edu.tw

S1. Power calculation for numerical simulation

The effect of the temperature on the ionic transport can be presented by chemical potential of the K^+ and Cl^- ions is given by [1]:

$$\overline{\mu}_i^j = \mu_i^{0,j} + RT^j \ln c_i^j + z_i F \phi^j , \tag{S1}$$

where $\mu_i^{0,j}$ is the standard chemical potential, c_i^j is the concentration, and ϕ^j is the inner potential of the ionic species *i*. Hence, the diffusion potential is given as

$$\phi_{diff} = \phi^H - \phi^L = \left(2t_+ - 1\right)\left(\frac{RT^H}{F} \ln c^H - \frac{RT^L}{F} \ln c^L \right), \tag{S2}$$

where the transference number (t_+) is given by

$$t_+ = \frac{I_{K^+}}{I_{K^+} + \left| I_{Cl^-} \right|} . \tag{S3}$$

The current can be calculated by integrating the ionic flux through the nanopore cross section. The current is obtained from ion species as:

$$I = F \sum_{i=1}^{4} \int_s \boldsymbol{J}_i z_i \boldsymbol{n} ds , \tag{S4}$$

where $\boldsymbol{n}$ is the unit normal vector of the cross-section of the nanopore. (Note that in performing the computation process, J_1, J_2, J_3, J_4 represent J_{K^+}, J_{Cl^-}, J_{H^+}, J_{OH^-}, respectively.) Having obtained the diffusion current and voltage, the power generation is given simply by

$$P = I \times V . \tag{S5}$$

The maximum power generation occurs when the open-circuit voltage V_{oc} and short-circuit current I_{sc} both have their half values, i.e.,

$$P_{\max\ power} = \frac{I_{sc} \times V_{oc}}{4} . \tag{S6}$$

S.2 Simulation setting

The ion concentration setting in boundary condition of reservoirs is adjusted based on pH level [2]. For pH> 7, $[K^+]=C_{K0}-10^{-(pH-3)}+ 10^{-(14-pH)+3}$ (mM), $[Cl^-]=C_{Cl0}$ (mM), $[H^+]=10^{-(pH-3)}$ (mM), $[OH^-]= 10^{-(14-pH)+3}$ (mM) (Assume that KOH is added into KCl solution to obtain pH>7). Similarly, for pH< 7, $[K^+] =C_{K0}$ (mM), $[Cl^-]=C_{Cl0} +10^{-(pH-3)}-10^{-(14-pH)+3}$ (mM), $[H^+]=10^{-(pH-3)}$ (mM), $[OH^-]= 10^{-(14-pH)+3}$ (mM) (Assume that HCl is added into KCl solution to obtain pH<7).

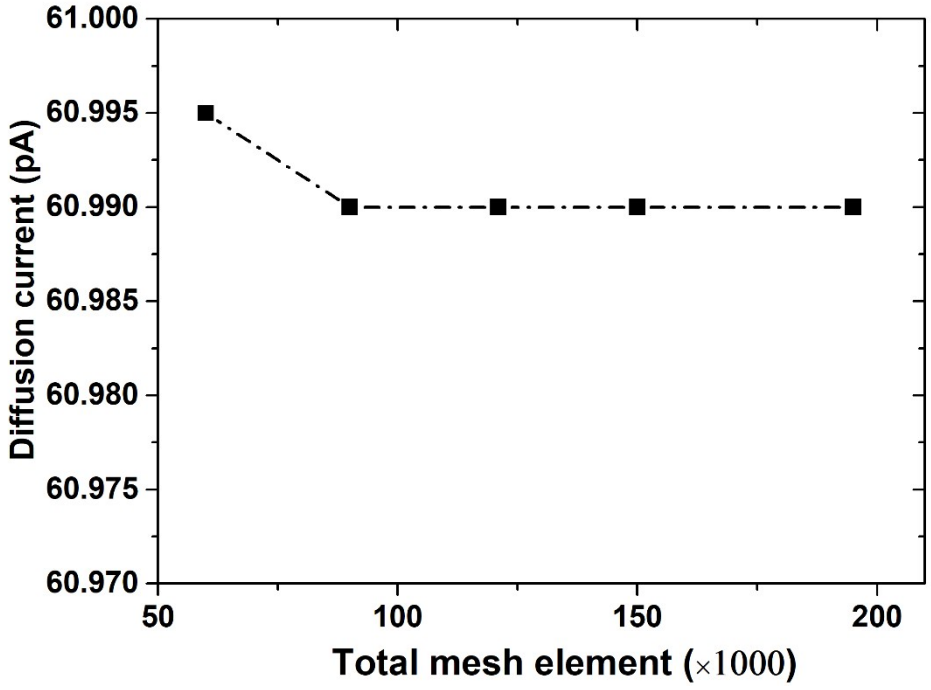

Figure S1: Diffusion current as function of mesh number. Note that the simulations consider a 1000-fold concentration gradient, a pore length of 500 nm. The model is meshed using quadratic elements. A finer mesh size is applied in the region of the electrical double layer (EDL). As shown in Fig. S1, a grid independence test was performed using meshing schemes consisting of 60,000 to 195,000 elements. Based on the simulation results, the mesh number was set in the model as 121,000.

Table S1: Boundary conditions for axisymmetric model.

Surface	Electric Potential	Ion Transport	Flow Field	Heat Transfer
AB	Constant voltage $\phi = V$	Low concentration	Pressure =0	T_R K
BC, FG	Zero charge $\boldsymbol{n}.\nabla\phi = 0$	No flux $-\boldsymbol{n}.\boldsymbol{J}_i = 0$	Slip	Thermal insulation
CD, EF	Zero charge $\boldsymbol{n}.\nabla\phi = 0$	No flux $-\boldsymbol{n}.\boldsymbol{J}_i = 0$	No slip	Thermal insulation
DE	Surface charge density $-\boldsymbol{n}\varepsilon_0\varepsilon_r\nabla\phi = \rho_s$	No flux $-\boldsymbol{n}.\boldsymbol{J}_i = 0$	No slip	Thermal insulation
GH	Ground	High concentration	Pressure =0	T_L K
HA	Axisymmetric	Axisymmetric	Axisymmetric	Axisymmetric

S.3 Effect of pH on surface charge density

Figure S1 shows surface charge varies with pH level in the range of 5 to 11. At pH 11, the surface charge density almost reaches to the basic charge (Eq.8). As pH level further reduces, the surface charge distribution reduces because of more protons in the nanopore.

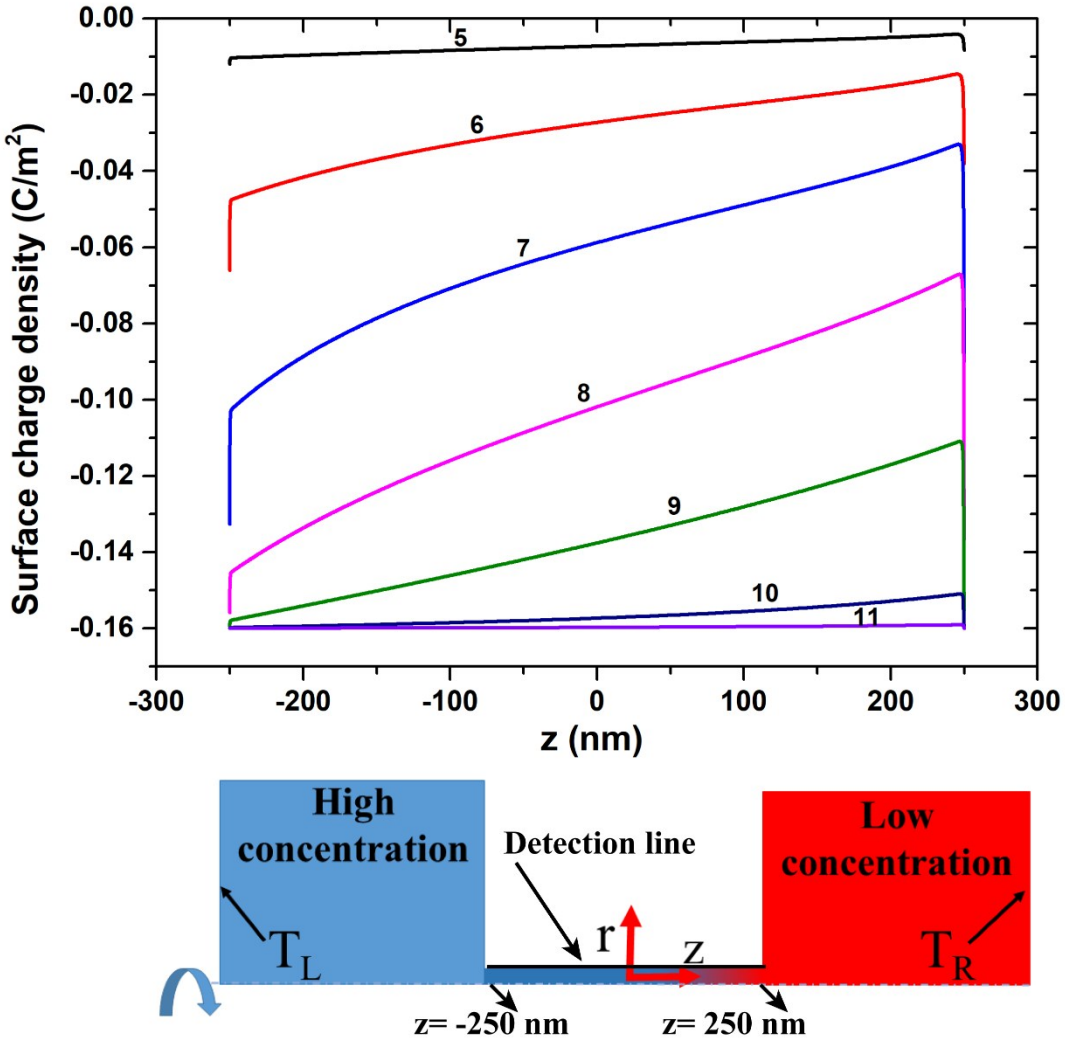

Figure S2: Surface charge density along nanopore varies with pH level in the range of 5~11.

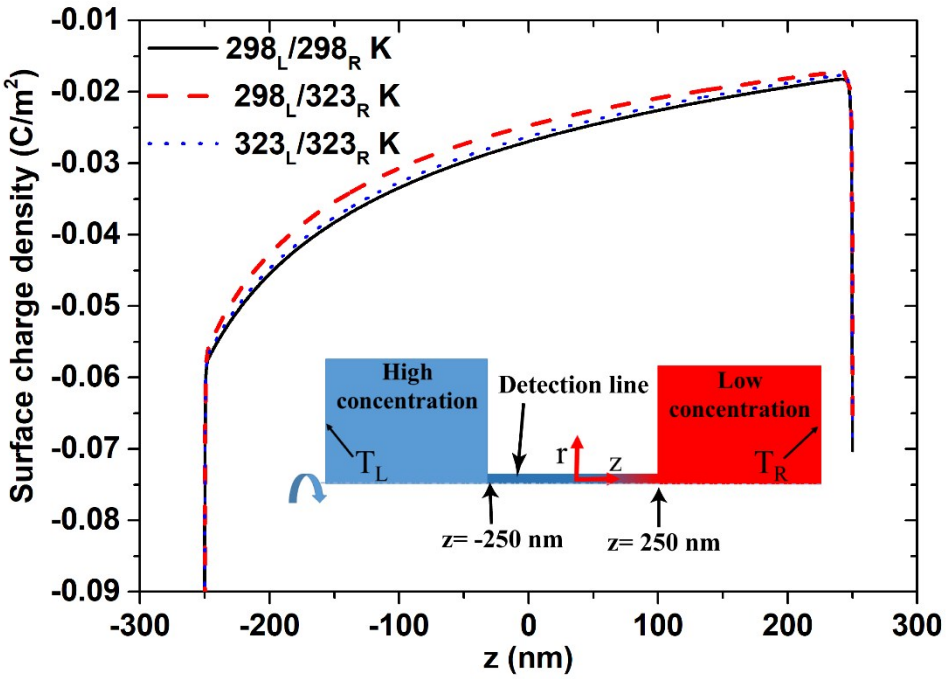

Figure S3: Surface charge density at 500 nm pore length, 100-fold concentration, and pH 7 in the case of open circuit voltage.

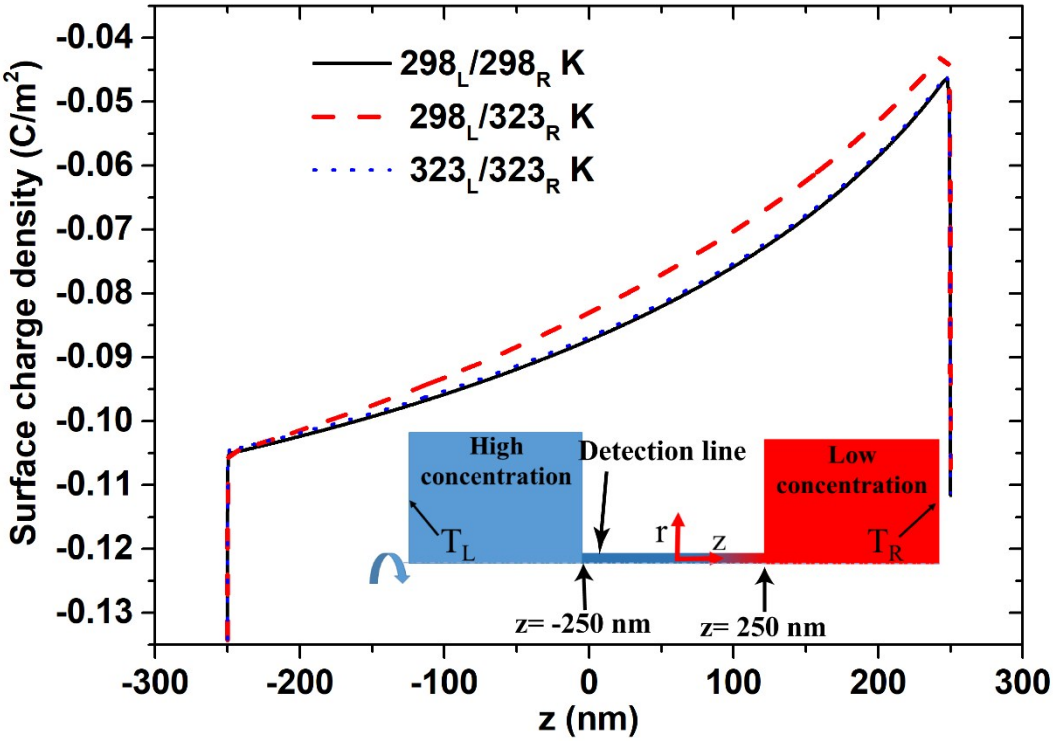

Figure S4: Surface charge density at 500 nm pore length, 1000-fold concentration, and pH 7 in the case of short circuit current.

S.4 Experimental verification of simulation method

The simulation results based on the coupled Poisson-Nernst Plank and Navier-Stokes equations (PNP-NS) were compared with the experimental data [3].

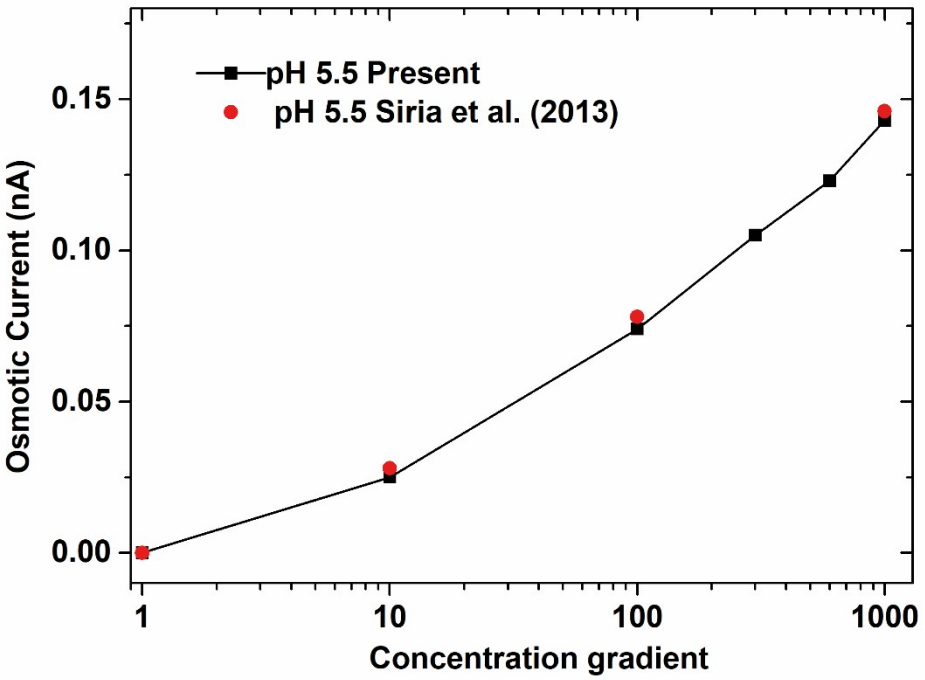

Figure S5: Comparison of simulation and experimental results for salinity gradient from 1-to 1000-fold. Note that experiment used boron nitride nanotube with diameter of 40 nm and length of 1250 nm. Note also that the results refer to a KCl solution with pH=5.5, hence, four species (K^+, H^+, Cl^- and OH^-) appeared in the system. The density of the chargeable sites is set as 18 sites/nm^2 in accordance with the prediction of Siria et al. [3].

S.5 Verification of simulation method based on coupled PNP-NS and heat transfer equations

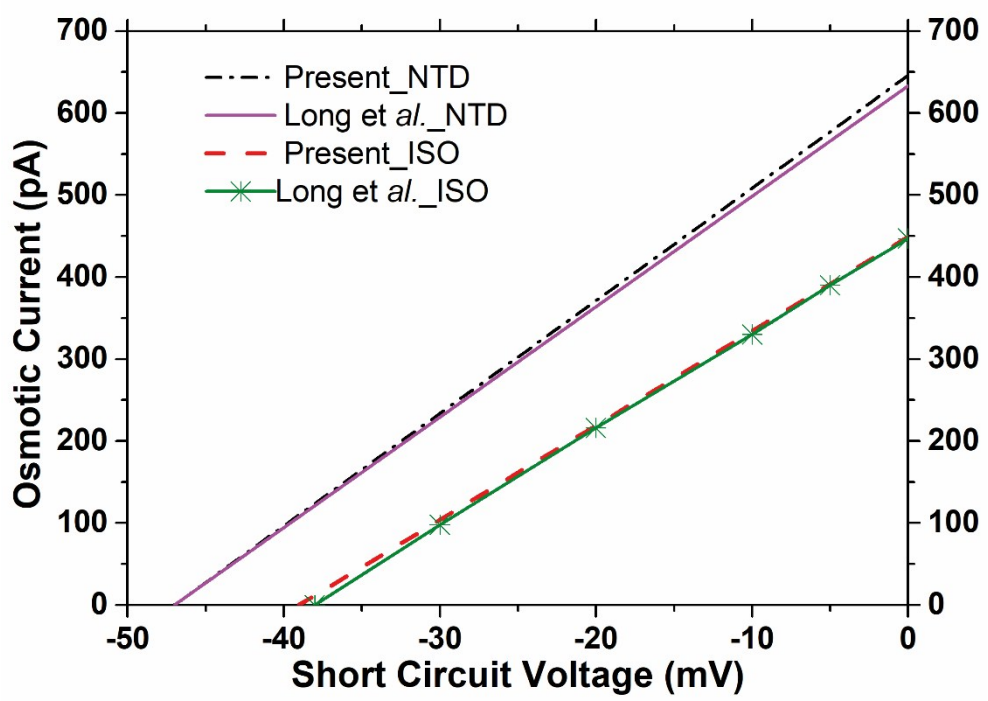

Figure S6: Comparison of simulation results reported by Long et al. (Note that the simulation based on coupling PNP-NS and heat transfer equations) [4]. Two simulation cases are considered, namely negative temperature difference (NTD) and isothermal (ISO). Note that a temperature difference of 20 K was set on the low-concentration reservoir side for the NTD case. For the isothermal case, a temperature of 298 K was set on both sides. In the simulation setting, the axisymmetric simulation model is used with a pore diameter and pore length of 10 nm and 50 nm, respectively.

S.6 Additional experiments

We conduct the experiments using polycarbonate track-etched membrane (6×10^8 pore cm^{-2}, effective area 0.785 cm^2 i.e., roughly million number of nanopores) to consider the effect caused by temperature difference on the blue energy harvesting. The effect of pH on the power generation had been reported in reference [2] but no thermal effect.

Figure S7 (a) shows the power generation under effect of 4 thermal conditions at pH 7, namely, (1) isothermal 298 K, (2) asymmetric thermal $298_L/323_R$ K, (3) Isothermal 310 K, (4) asymmetric thermal-switching direction $323_L/298_R$ K. The asymmetric thermal case $298_L/323_R$ K (higher temperature is set on low-concentration reservoir) presents the highest power generation in comparing to the other three cases. In the case of asymmetric thermal-switching direction $323_L/298_R$ K (higher temperature is set on high-concentration reservoir), there is no improvement of power generation compared to isothermal 298 K. It supports the finding shown in Fig. 2 in the main text, in which high temperature at high-concentration reservoir has no contribution in improving nanopore performance. Besides, the power generation of isothermal 310 K case is 38 % smaller than that of case 2- asymmetric thermal $298_L/323_R$ K, even the energy cost is nearly the same in these two cases.

Figure S7 (b) shows the power generation as function of temperature difference δT in the range of 0- 36 K. As δT increases from 0 to 25 K, the obtained power generation increases proportionally. However, the power saturates as δT further increases to 36 K. Fig. S7 (b) experimentally supports to the simulation result shown in Fig. 7(a) in the main text.

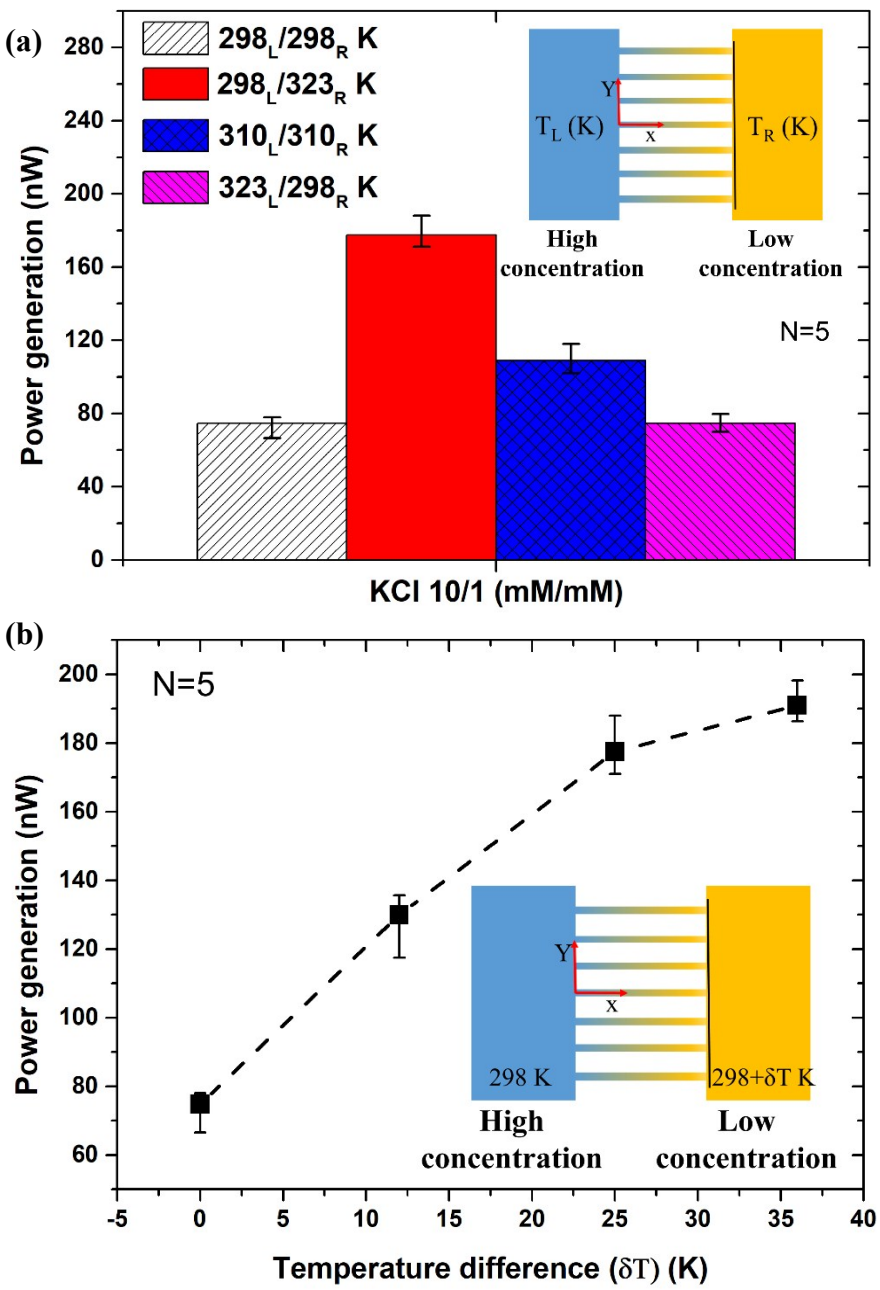

Figure S7: (a) power generation under effect of 4 thermal conditions at pH 7 (1) Isothermal 298 K, (2) asymmetric thermal $298_L/323_R$ K, (3) Isothermal 310 K, (4) asymmetric thermal-switch direction $323_L/298_R$ K. (b) power generation as function of temperature difference δT.

References of Supporting Information

1. K. Chen, L. Yao and B. Su, *J. Am. Chem. Soc.*, 2019, **141**, 8608-8615.

2. J.-P. Hsu, T.-C. Su, P.-H. Peng, S.-C. Hsu, M.-J. Zheng and L.-H. Yeh, *ACS nano*, 2019, **13**, 13374-13381.

3. A. Siria, P. Poncharal, A.-L. Biance, R. Fulcrand, X. Blase, S. T. Purcell and L. Bocquet, *Nature*, 2013, **494**, 455.

4. R. Long, Z. Kuang, Z. Liu and W. Liu, *Natl. Sci. Rev.*, 2019, DOI: 10.1093/nsr/nwz106, 10.1093/nsr/nwz1106.